ISME

www.nature.com/ismej

ARTICLE

Permissive aggregative group formation favors coexistence between cooperators and defectors in yeast

Tom E. R. Belpaire[1,2✉], Jiří Pešek[3], Bram Lories[2], Kevin J. Verstrepen[2,4], Hans P. Steenackers[2], Herman Ramon[1] and Bart Smeets[1]

In *Saccharomyces cerevisiae*, the *FLO1* gene encodes flocculins that lead to formation of multicellular flocs, that offer protection to the constituent cells. Flo1p was found to preferentially bind to fellow cooperators compared to defectors lacking *FLO1* expression, enriching cooperators within the flocs. Given this dual function in cooperation and kin recognition, *FLO1* has been termed a "green beard gene". Because of the heterophilic nature of the Flo1p bond however, we hypothesize that kin recognition is permissive and depends on the relative stability of the $FLO1^+/flo1^-$ versus $FLO1^+/FLO1^+$ detachment force F. We combine single-cell measurements of adhesion, individual cell-based simulations of cluster formation, and in vitro flocculation to study the impact of relative bond stability on the evolutionary stability of cooperation. We identify a trade-off between both aspects of the green beard mechanism, with reduced relative bond stability leading to increased kin recognition at the expense of cooperative benefits. We show that the fitness of *FLO1* cooperators decreases as their frequency in the population increases, arising from the observed permissive character ($F_{+-} = 0.5\,F_{++}$) of the Flo1p bond. Considering the costs associated with *FLO1* expression, this asymmetric selection often results in a stable coexistence between cooperators and defectors.

The ISME Journal (2022) 16:2305–2312; https://doi.org/10.1038/s41396-022-01275-y

INTRODUCTION

The transition towards multicellularity is one of the major developments that has driven the evolution of complex life [1–3]. Initially, independent individuals form facultative cooperative groups which can serve as a starting point for the evolution of obligate multicellular organisms wherein the individuals lose the ability to replicate independently [4–6]. These facultative groups can be formed through two distinct operations: formation of aggregative groups, known as "coming together" (CT), and clonal growth, where the offspring remains closely associated with the parental cell, known as "staying together" (ST) [4, 7, 8]. ST gives rise to clonal groups with high genetic relatedness whereas CT may also result in genetically mixed groups.

In featuring both unicellular lifestyles and various group phenotypes, *Saccharomyces cerevisiae* serves as a paradigm for studying ST [9–12] and CT [13–15] group formation, although *S. cerevisiae* does not have any known obligate multicellular descendants [4]. A key gene family involved in group formation in yeast comprises the *FLO* genes, which encode for flocculins, proteins involved in cell adhesion [4, 13, 16–20]. These flocculins possess an N-terminal domain protruding from the cell surface, a central domain of tandem repeated sequences, and a C-terminal glycosylphosphatidylinositol (GPI) domain anchored in the cell wall [16, 21]. Based on the N-terminal domain, two types of flocculins can be distinguished. Flo11p harbors a fibronectin type III-like domain that confers homophilic protein-protein interaction with neighbouring cells [12, 22]. Flo11p-mediated adhesion partakes in multiple ST group phenotypes such as biofilm [12, 23, 24] and pseudohyphae formation [25]. In contrast, the *FLO1* gene encodes for a PA14-like N-terminal domain that binds to mannose residues on the cell wall of neighbouring cells, a mechanism that is heterophilic in nature [26, 27]. Flo1p controls the CT flocculation phenotype, causing yeast cells to aggregate and form flocs in agitated suspensions. When sufficiently large, these flocs offer protection to the constituent cells against chemical [13] and biological [28, 29] stress. Furthermore, flocs ensure rapid sedimentation to escape undesirable conditions [30]. As such, floc formation is a type of cooperative behavior in which the benefit only exists when sufficient individuals participate [13].

In addition to facilitating group formation, both types of *FLO* genes also permit kin recognition through selective adhesion. In this quality, they have been identified as "green beard genes", a single set of alleles that promotes cooperation while also excluding non-collaborating individuals (defectors) [13, 31, 32]. In case of *FLO11* selective adhesion is mediated by the homophilic nature of the interaction [12]. Flo1p was also found to preferentially bind to fellow cooperators compared to defectors, resulting in enrichment of cooperators within the flocs [13]. The heterophilic nature of the Flo1p bond however also permits adhesion to non-producer cells. The observed enrichment of cooperator cells might then be explained by a higher bond strength between cooperators due to the potential of reciprocity in homotypic $FLO1^+/FLO1^+$ interactions. We hypothesize that kin recognition via such heterophilic attachment is however only

[1]Division of Mechatronics, Biostatistics, and Sensors, KU Leuven, 3001 Leuven, Belgium. [2]Centre for Microbial and Plant Genetics, KU Leuven, 3001 Leuven, Belgium. [3]Team SIMBIOTX, Inria Saclay, 91120 Palaiseau, France. [4]Laboratory of Systems Biology, VIB-KU Leuven Center for Microbiology, 3001 Leuven, Belgium.
✉email: tom.belpaire@kuleuven.be

Received: 6 January 2022 Revised: 8 June 2022 Accepted: 16 June 2022
Published online: 1 July 2022

partially selective and dependent on the relative stability of *FLO1*$^+$/*flo1*$^-$ versus *FLO1*$^+$/*FLO1*$^+$ interactions, which itself depends on the intrinsic bond properties but also the tensile forces trying to separate interacting cells. Since *S. cerevisiae* lacks intrinsic motility, shear forces arising due to fluid flow are thought to be the main instigators of bond formation and breakage events. Because of this potentially'permissive' nature of the *FLO1* kin recognition, defectors might still be able to invade flocs and exploit the benefits of cooperation [12, 15]. Since defectors do not pay the metabolic cost associated with Flo1p production, they can potentially outgrow the cooperators. Consequently, the evolutionary stability of *FLO1* is not guaranteed. Knowing the impact of relative bond stability and its driving factors on kin recognition is therefore critical to understand the evolution of CT flocculation driven by heterophilic Flo1p adhesion.

In this work, we evaluate the impact of the relative bond stability of heterotypic and homotypic Flo1p interactions on the exclusion of defectors and the evolutionary stability of flocculation in mixed populations with varying cooperator frequencies. To this end, we first determine the intrinsic relative stability of heterotypic and homotypic interactions using single cell-force spectroscopy (SCFS) and subsequently characterize the extent of permissiveness in Flo1p-mediated kin recognition. Based on these measured bond properties, we evaluate both the cooperative benefits and the degree of kin recognition of the *FLO1* green beard cooperation and its evolutionary stability using cell-based simulation of shear-induced CT group formation. We conclude that the relative stability of heterotypic and homotypic interactions, modulated by varying either tensile shear stresses or bond properties, determines a trade-off between kin recognition and cooperative benefits. Remarkably, size-dependent selection of clusters results in a decrease in overal fitness of cooperators as their frequency increases, which stabilizes coexistence between defectors and cooperators in a broad range of ecological and mechanical conditions. Stable coexistence ensures the retention of diversity and thus facultative group formation, which might eventually give rise to evolution of obligate multicellularity.

MATERIALS AND METHODS

Yeast strains and media

Yeast strains (Table S1) were first cultured in YPD for 3 days and subsequently inoculated in YPG and grown for 2 days. Afterwards, cells were harvested and washed once in 200 mM EDTA and twice in Milli-Q water. In case of *FLO1*$^+$, flocculation was governed by expression of the *FLO1* gene from the nonflocculent laboratory strain S288C under transcriptional control of the GAL1 promoter. *flo1*$^-$ has an identical resistance gene marker, but did not show flocculation due to absence of the promoter.

Single-cell force spectroscopy

Single-cell force spectroscopy was performed as described by [26]. In short, cell probes were prepared by immobilizing single yeast cell on polydopamine-functionalized tipless cantilevers. The cell probe was brought into contact with single cells immobilized on a glass coverslip with polydopamine using a maximum contact force of 1 nN, retract velocity of 1 μm/s and contact time of 1 s in the presence of 200 μM $CaCl_2$. Cell viability of both the cell probe and the immobilized cells on the substrate were followed by the FUN-1 cell stain throughout the measurement.

Flocculation assays

After harvesting and washing yeast cells at various ratios of *FLO1*$^+$ and *flo1*$^-$, cells were inoculated in 5 ml Milli-Q water with a final density of $3.0 \pm 1.4\ 10^6$ cells/mL. After inoculation the tubes were carefully turned to homogenize them and sampled for the initial ratio of cells x_i. Test tubes were shaken on an orbital shaker at varying agitation rates (0, 100, 200, or 400 RPM) for 5 min. After agitation, the flocs were allowed to settle for 5 min after which the sedimented fraction was sampled x_{out}. Prior to cell counting using flow cytometry, samples were washed with 200 mM EDTA to disrupt any floc formation. Ratios x were determined as the fraction of red *FLO1*$^+$ cells versus the total amount of cells. The experiments were performed in 10 mM $CaCl_2$ necessary for flocculation, and in Milli-Q water as a control.

Individual cell-based model

We performed simulations of a center-based cell model in an overdamped system in laminar flow with periodic boundary conditions in the direction of the laminar flow. The boundaries perpendicular to the flow direction are reflective. External shear force is imposed based on a set shear rate $\dot{\gamma}$. Cell-cell interaction was modeled using a linear adhesion model with rupture force F_d and rupture distance d_r, Hertzian repulsion and linear intercellular viscosity. Cell velocities v were computed by solving $F = \Lambda v$, with Λ the combined friction/resistance matrix. Positions are updated according to the explicit Euler method. A full description of the computational methods is given in the SI text, as well as the parameters used in the simulations (Table S3).

RESULTS

Flo1p confers heterophilic cell-cell adhesion

Flo1p flocculins bind to mannose residues on neighbouring cells. To quantify the cell-cell interaction force resulting from these adhesive bonds, we employ the SCFS method described by El-Kirat-Chatel et al. [26]. We test three types of interaction pairs: *flo1*$^-$/*flo1*$^-$, *FLO1*$^+$/*flo1*$^-$, and *FLO1*$^+$/*FLO1*$^+$. We measure the detachment force F_d and the rupture distance d_r of every cell-cell interaction type (Fig. 1A–F). Based on the maximal measured detachment forces (see Supplementary Information), we estimate that the cell surface density of FLO1p is approximately ≈380 FLO1p μm^{-2}. In addition, the mean detachment force F_{+-} of the heterotypic interaction is approximately half (≈55%) of the mean homotypic *FLO1*$^+$ interaction, whereas a homotypic *flo1*$^-$ interaction is an order of magnitude lower in adhesive strength, ≈7% of the mean homotypic *FLO1*$^+$ detachment force. This heterophilicity in cell-cell interaction is consistent with a permissive kin recognition mechanism [15].

To evaluate the effect of permissive kin recognition on the community structure of yeast aggregates, we consider the differential adhesion hypothesis (DAH), which predicts the thermodynamic equilibrium configuration of a mixture of cells based on the interaction energy of possible cell type pairings. For a binary mixture, the DAH predicts three different modes of organization: (i) segregation, where both cell type preferentially interact homotypically (ii) spreading, where the low adhesive cell type engulfs cores of the highly adhesive cell type and (iii) intermixing, where both cell types preferentially interact heterotypically [33]. In our case the DAH predicts spreading of *flo1*$^-$ cells around the *FLO1*$^+$ cells based on the heterotypic and respective homotypic interaction energies, here defined as $E = F_d d_r/2$. Spreading of *flo1*$^-$ cells around a central *FLO1*$^+$ cluster has previously been observed and produces additional benefits in macroscopic flocs. For example, in the case of protection against antifungal compounds such as amphotericin B, the outer layer of *flo1*$^-$ cells can serve as "living shield", leading to increased protection of the *FLO1*$^+$ cells at the core of the floc [13]. In contrast, the absence of segregation indicates potential for exploitation of the flocculation by the *flo1*$^-$ cells, as segregation is thought to be the ideal scenario for cooperative phenotypes [34–36]. As stated above, the DAH predicts the configuration of a mixture of cells at thermodynamic equilibrium. However, yeast cells are too large to be significantly agitated by thermal forces, and they lack intrinsic cell motility. Consequently, in real-life conditions, substantial energy barriers can prevent the system from relaxing to its equilibrium configuration. Hence, to evaluate the degree of kin recognition due to *FLO1* expression, the driving forces responsible for floc formation must be taken into account.

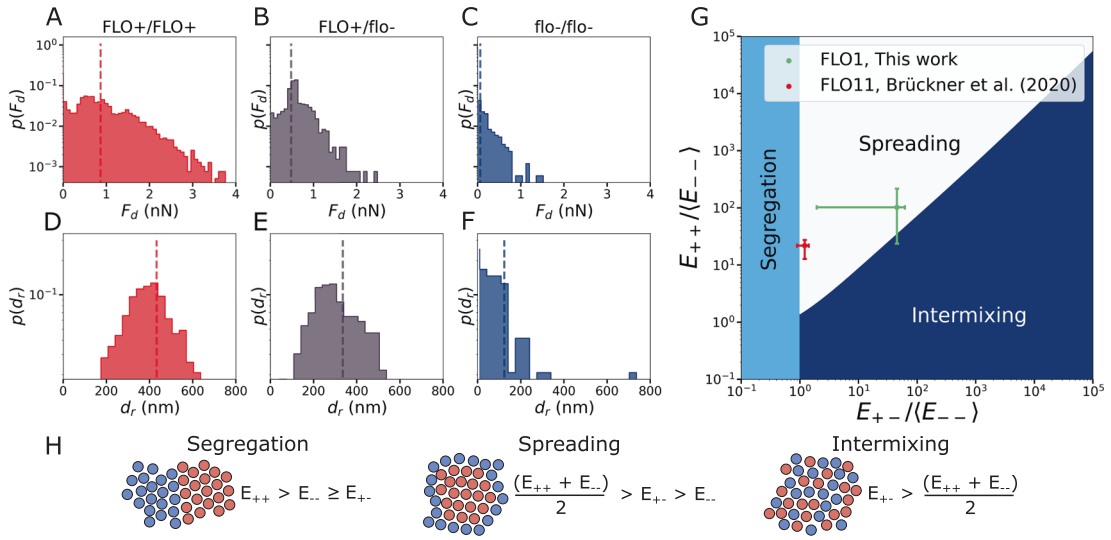

Fig. 1 Mechanical measurement of Flo1p bond properties and mixing predictions. Probability density functions of the measured maximum detachment force F_d for **A** *FLO1*$^+$/*FLO1*$^+$ ($n = 1567$, 6 cell interaction pairs), **B** *FLO1*$^+$/*flo1*$^-$ ($n = 1311$, 6 cell interaction pairs) and **C** *flo1*$^-$/*flo1*$^-$ interactions ($n = 905$, 6 cell interaction pairs). The dotted lines indicate the mean detachment forces. **D–F** Probability density function of the rupture length d_r of cell-cell interaction, measured by maximum distance with significant adhesive forces. The dotted lines indicate the mean rupture lengths. **G** Based on the bond energies, $E = F_d d_r/2$, the colony structure was predicted by the differential adhesion hypothesis (DAH). Single cell-force spectroscopy data of Flo11p was obtained from [12]. Dots indicate the median energy, bars indicate the 25th and 75th quantile. **H** DAH predicts segregation, spreading, and intermixing based on the ratio of bond energies.

Shear flow promotes relatedness in mixed clusters at the expense of cooperative benefits

Flocs originate from collisions between individual yeast cells, which are facilitated by external forces, such as shear forces arising due to fluid flow. In practice, the formation of large flocs is realized in two stages: (1) nucleation and growth of small clusters due to collisions in shear flow and (2) differential sedimentation and size-based separation of clusters, leading to macroscopic flocs. Based on the observed mean detachment forces and rupture lengths, we evaluate the size and composition of cell clusters in a minimal linear shear simulation with varying initial cooperator frequency x_i and shear rate $\dot{\gamma}$ (Fig. 2A–E). It is reasonable to assume that the main benefit of cooperation is increased cluster size, potentially conferring faster sedimentation [9, 14, 37], increased protection against chemicals [13], and predators [7, 28, 38, 39]. At sufficient cell density, the average cluster size C shows an exponential shear-dependent relaxation over time towards a dynamic steady-state. In contrast, at low density, a slowed-down relaxation is observed, indicative of granular compaction in between infrequent collision events (Fig. 2F, S1). In both density regimens, the steady-state cluster size C_∞ decreases with shear rate. Moreover, cluster size increases with the initial fraction of cooperators (Fig. 2G).

To evaluate the selectivity of *FLO1*, we consider the cell type composition of clusters after flocculation. Overall, enrichment of *FLO1*$^+$ cells is observed in clusters, which increases with shear rate as heterotypic interactions become unstable at lower shear rates than homotypic interactions (Fig. 2H, S5). However, due to the permissive binding mechanism, selection for *FLO1*$^+$ is weak. This is further apparent in the relatedness $r = \left(\langle p_i^2\rangle - \langle p_i\rangle^2\right)/\left(\langle p_i\rangle - \langle p_i\rangle^2\right)$, where $\langle p_i\rangle$ indicates the cooperator fraction per cluster averaged over all clusters, and is thus evaluated at the level of whole clusters rather than the level of single cells and their direct neighbours. Relatedness signifies the directness of cooperative interactions, with $r = 1$ in populations with clusters uniquely composed of *FLO1*$^+$ or *flo1*$^-$ cells and $r = 0$ in absence of variation in cluster composition [40]. In general, we find only modest relatedness ($r < 0.3$) in all shear regimens, characteristic for CT group formation and permissive kin recognition [40, 41]. Nonetheless, relatedness is favored by increasing shear rate (Fig. 2I, S5). Finally, we also observe radial assortment within clusters, where *FLO1*$^+$ cells are predominantly at the central core and *flo1*$^-$ cells more towards the outer edges, as was also noted by Smukalla et al. [13] in much larger flocs, and in line with the equilibrium conditions predicted by the DAH (Fig. S6). However, this assortment is not very pronounced, and these micro-assorted clusters are too small to provide protection to realistic chemical stress conditions. In conclusion, shear-driven aggregation of mixtures of cooperators and defectors leads to partially selective group formation due to the exclusion of defectors from clusters, which results in smaller but more selective clusters with increasing shear rate. However, selection is not very efficient due to the permissive binding mechanism of Flo1p that allows for a heterogeneous cluster composition at all shear conditions, and is different from the thermodynamical equilibrium predicted by DAH (Fig. 1G).

Permissive kin recognition facilitates coexistence

The evolutionary robustness of *FLO1* depends on its associated costs and benefits. We evaluate both by using a conceptual modeling framework consisting of three sequential ecological processes (Fig. 3A). First, a mixed population with cooperator frequency x_i is exposed to shear flow and allowed to flocculate (Fig. 2). Second, cells are selected based on the steady-state cluster size C_∞, and thus the expected benefit offered by the cluster they belong to. The probability to survive is $P(survive) = 1 - exp[-C_{t,final}^{2/3}/(\alpha C_{(\infty|x_i=1)}^{2/3})]$, with $C_{(\infty|x_i=1)}$ mean cluster size for a fully cooperative system and α a parameter tuning the selection strength. P(survive) is based on the Stokesian sedimentation velocity $v_i \propto C_i^{2/3}$ i.e., larger clusters sediment faster and have an increased selection probability (Fig. 3B, S7). Third, the selected cells are allowed to grow exponentially until the next flocculation event [42, 43], taking into account a 3% percent growth deficit for the *FLO1*$^+$ cells relative to the *flo1*$^-$ cells (Fig. 3C) [13]. After flocculation, selection, and growth, the cooperator enrichment Δx_i is determined based on the frequency of cooperators before and after each of the three steps, $\Delta x_i = x_{\text{out}} - x_i$.

After flocculation and selection (thus prior to the growth step), there is a preferential retention of cooperating cells for $\alpha > 0$. The peak in cooperator enrichment Δx_i after selection showcases an asymmetry towards a lower cooperator frequency (Fig. 3B, S8). At

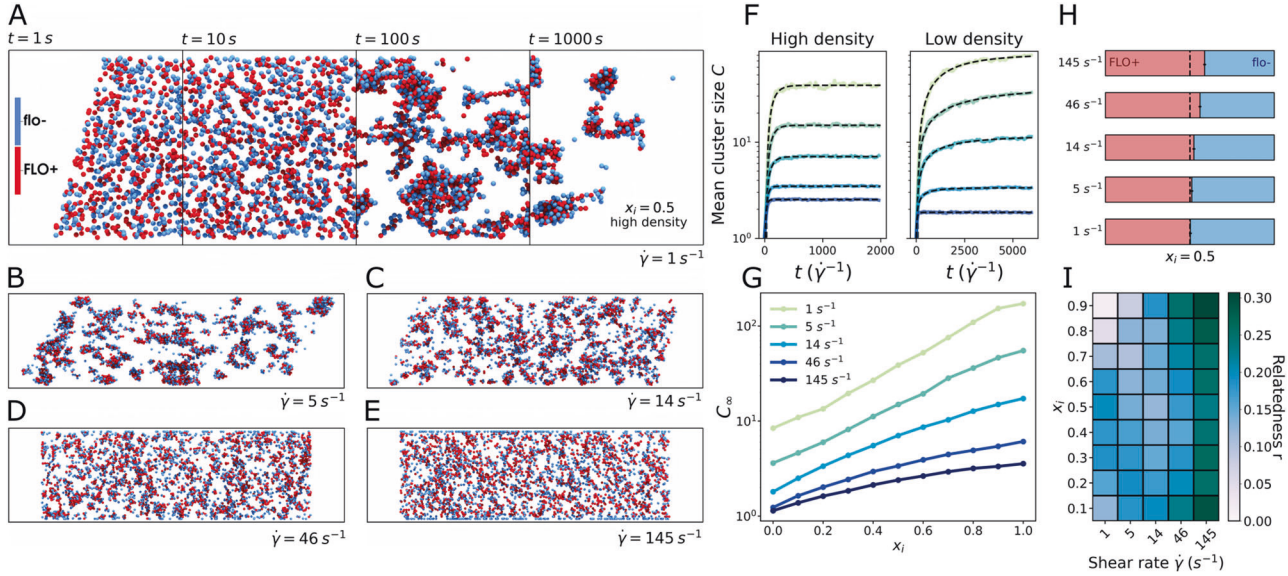

Fig. 2 Effect of shear on heterotypic Flo1p-dependent flocculation. A Temporal progression of flocculation starting from a homogeneously mixed population of *FLO1*$^+$ (red) and *flo1*$^-$ (blue) at increasing time points $\dot{\gamma}t$, shown for a cooperator frequency $x_i = 0.5$, high density, $\rho_{high} = 1.66 \times 10^7$ cells/ml and shear rate $\dot{\gamma} = 1\ s^{-1}$. **B**–**E** Endpoint of flocculation at various shear rates, shown for cooperator frequency $x_i = 0.5$. **F** Time evolution of the mean cluster size C for high ($\rho_{high} = 1.66 \times 10^7$ cells/ml) and low density ($\rho_{low} = 0.83 \times 10^7$ cells/ml) for varying shear rate (color legend identical to **G**). The black lines indicate exponential fit $C(t) = C_\infty[1 - \exp(-t/\tau)]$ and a stretched exponential $C(t) = C_\infty[1 - \exp(-(t/\tau)^\beta)]$ fit for the high and the low density respectively. At high ("super-critical") density, the projected area, integrated across a circular flow line is larger than one, and the system reaches a dynamic steady-state. At low ("sub-critical") density, this projected area is lower than one, and collisions become exceedingly rare after closed flow lines have been depleted of cells, see also Supplementary Figs. S1, S2. **G** Mean steady-state cluster size C_∞ in function of cooperator frequency x_i for varying shear rate, see also Supplementary Fig. S3. **H** Cluster composition for clusters of size > 2 cells for varying shear rate. The dotted black line indicates cooperator frequency $x_i = 0.5$. Bars indicate standard deviation. **I** Cluster relatedness in function of shear rate $\dot{\gamma}$ and cooperator frequency x_i, see also Supplementary Figs S4, S5. The mean of four independent simulation repeats is shown ($n = 4$).

low x_i, only clusters with a frequency of cooperators $\gg x_i$ are sufficiently strong to resist the disruptive force from shear flow. This results in a relative enrichment of cooperators in the surviving clusters. Conversely, at large x_i, the abundance of cooperators in clusters provides sufficient favorable locations for defector cells to be incorporated and the frequency of cooperators in clusters approaches the initial population frequency. Upon imposing a growth-associated cost for cooperation, this asymmetry can result in selection in favor of cooperators at low x_i ($\Delta x > 0$) and selection for defectors at high x_i ($\Delta x < 0$) (Fig. 3C).

Based on the shape of the cooperator enrichment curve, we determine the evolutionarily stable strategy (ESS) as a function of selection strength α ($\propto$ social benefits) and growth time in between flocculation events ($\propto$ social cost), and this at varying shear rate (Fig. 3D). Cooperation emerges as an ESS for increasing strength α. However, given a high growth time in between flocculation—or high growth-associated costs—the resulting ESS is defection. This highlights that permissive kin recognition due to heterophilic cell-cell attachment is not efficient at fully excluding defector cells from cooperative groups without additional external selection pressure [15]. However, due to the aforementioned asymmetry in selection, coexistence is the ESS for a large range of ecological parameters. The stable point (i.e., the stable frequency of cooperators) shifts towards a lower cooperator frequency with higher growth time between flocculation events (Fig. S9). Whereas cooperation is more favored with increasing shear rate, coexistence is notably favored at intermediate shear rate, where the asymmetry in selection is most pronounced (Fig. S8). Here, cooperative homotypic cell-cell interactions are always stable, whereas permissive heterotypic interactions can be broken by tensile shear forces, thereby maximizing the relative enrichment of cooperators at low x_i. Finally, at low cell density, clusters are more compact and collide less frequently compared to high cell density. Consequently, the peak in coexistence shifts towards higher shear rate, as more shear force is required to penalize the incorporation of permissive interactions in dense, well-connected clusters (Fig. S1).

For in vitro verification of the predicted asymmetric cooperator enrichment, we mimic the first two steps of the evolutionary framework, flocculation, and selection, using a simple flocculation-sedimentation assay, where we inoculate various cooperator fractions and agitate them at varying rotator speed. Selection is performed by sampling from the sediment, which contains flocs that preferentially consist of larger clusters (Fig. S10). Based on the frequency of cooperators in the sedimented (i.e., selected) flocs and the inoculum frequency, the cooperator enrichment is determined (Fig. 3E). Increasing the rotor speed ($\propto$ shear rate) resulted in increasingly positive cooperator enrichment curves in the presence of Ca^{2+}—which is required for flocculation—indicating an increased exclusion of *flo1*$^-$ cells, as observed in silico (Fig. 2). In addition, at sufficient rotor speed (200 RPM and 400 RPM) the maximal enrichment is located at a lower cooperator frequency, demonstrating the same characteristic asymmetry in *FLO1*$^+$ enrichment that was predicted from in silico simulations (Fig. 3B). When including a fixed cost incurred by growth, these cooperator enrichment curves will give rise to coexistence as an ESS for a mixed population of *FLO1*$^+$ and *flo1*$^-$ cells (Fig. 3D).

Flo1p bond mechanism permits evolutionary flexibility

The emergence of coexistence due to asymmetric selection is contingent on permissive interactions and is absent in a hypothetical scenario with direct kin recognition where $F_{+-} = F_{--}$. In case of direct kin recognition, symmetrical cooperator enrichment Δx_i expands the fully cooperative region at the expense of coexistence (Fig. 4A, B). Due to extensive exclusion of defector cells from clusters, cooperation remains stable at a much higher number of growth time

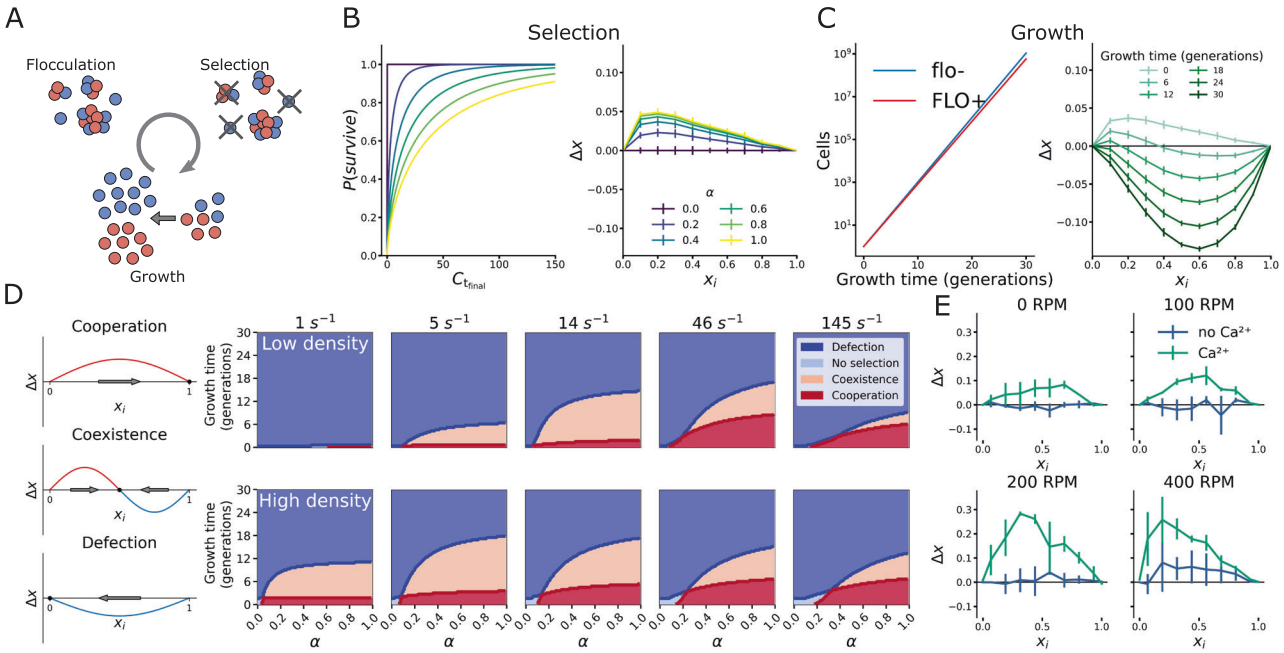

Fig. 3 Population dynamics in *FLO1* cooperation. A Three sequential ecological processes are considered; flocculation, selection by sedimentation and growth. **B** Cluster size selection probability P(survive) in function of steady-state cluster size $C_{t,\text{final}}$. Cooperator enrichment Δx after selection at varying selection strength α is shown for $\dot{\gamma} = 14\,s^{-1}$. **C** selected *FLO1*$^+$ cells experience a growth deficit relative to *flo1*$^-$ of 3% as reported by Smukalla et al. [13]. Cooperator enrichment curves at moderate selection strength ($\alpha = 0.4$, $\dot{\gamma} = 14\,s^{-1}$) and increasing growth time expressed as generations which are the number of population doublings of *flo1*$^-$ cells in between successive flocculation events. The mean and standard deviation of four independent simulation repeats is shown ($n = 4$). (**D**) Classification of cooperator enrichment curves in evolutionarily stable strategies (ESS) cooperation, coexistence, defection. ESS in function of α and growth time between successive flocculation events for high and low density, see also Supplementary Fig. 2. (**E**) Experimental characterization of cooperator enrichment for various rotor amplitudes in the presence and absence of Ca^{2+}. The mean and standard deviation of three independent experimental repeats are shown ($n = 3$).

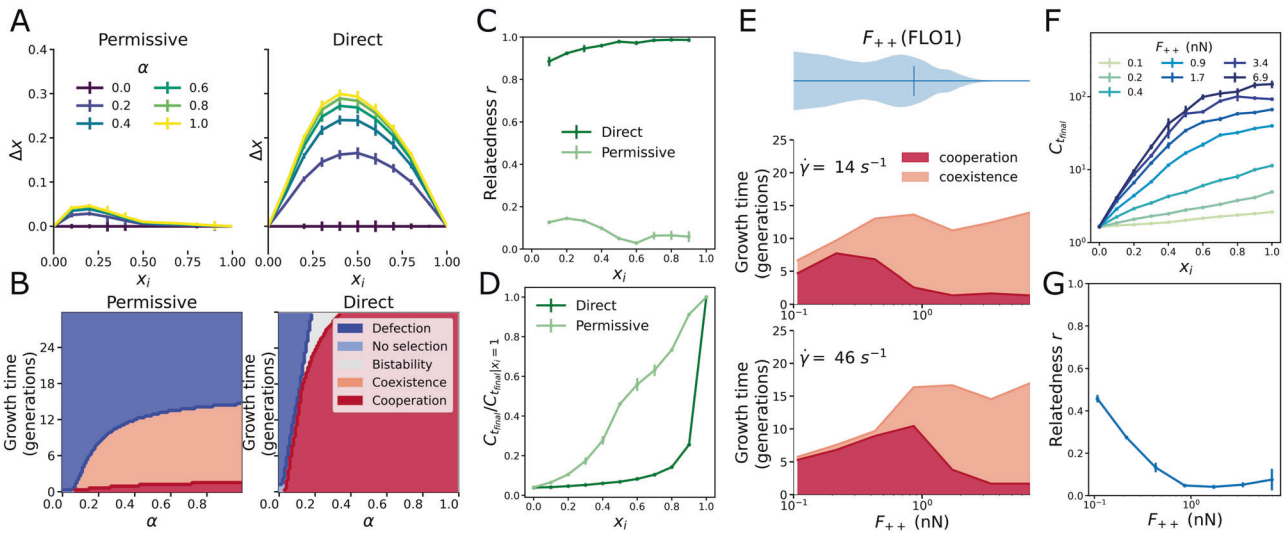

Fig. 4 Effect of Flo1p bond properties on evolutionary stability. A Cooperator enrichment Δx after flocculation and selection for permissive and direct kin recognition. **B** Evolutionarily stable strategy (ESS) for permissive and direct kin recognition. For direct kin recognition, bistability emerges when Δx is increasing at the zero point [50]. **C** Relatedness r in function of initial cooperator frequency x_i for permissive and direct kin selection. **D** Cooperative benefits relative to the fully cooperative system $x_i = 1$ for both permissive and direct kin recognition. **E** Empirical *FLO1*$^+$/*FLO1*$^+$ detachment force variability F_d. Effect of bond strength on the ESS at strong selection ($\alpha = 1$). **F** Final cluster size $C_{t\text{final}}$ in function of initial cooperator frequency x_i for varying homotypic detachment forces F_{++}, conserving $F_{++} \approx 2\,F_{+-}$. (**G**) Relatedness r in function of F_{++}, conserving $F_{++} \approx 2\,F_{+-}$ shown for $x_i = 0.5$. Results are shown for low density ($\rho_{\text{low}} = 0.83 \times 10^7$ cells/ml) and shear rate $\gamma = 14\,s^{-1}$. The mean and standard deviation of three independent simulation repeats are shown (n=3).

in between flocculation events (Fig. 4B, C). Remarkably, the exclusion of defector cells in direct kin recognition also results in smaller clusters, and thus cooperation-associated benefits, in mixed populations ($0 < x_i < 1$) (Fig. 4D). Moreover, since the cooperation-associated benefits are small at low x_i, the emergence of direct kin recognition, e.g., by mutation of a single cell, is not expected to perpetuate in an initially fully defective population ($x_i = 0$) in CT group formation. In contrast, permissive recognition is more favorable to develop due to higher cooperation-associated benefits and asymmetric cooperator enrichment. In exchange for the resistance to defection provided by the increased selectivity of direct kin recognition, the permissiveness of the Flo1p bond permits evolutionarily stable flexibility, by conserving coexistence between cooperators and defectors.

In contrast to the hypothetical nature of direct kin recognition due to the Flo1p bond mechanism, variability in adhesive strength in flocculation has been observed to arise due to stochasticity in bond formation (Fig. 1A–C, Fig. 4E), or variation in the intragenic tandem repeats of *FLO1*, which are known to undergo frequent recombination events [19, 26]. Varying the homotypic adhesive strength F_{++} while conserving the ratio $F_{++} \approx 2\,F_{+-}$ highlights the dilemma of a permissive green beard gene: In case of an increase in adhesion, the cooperative benefits increase (Fig. 4F, S11), but this weakens kin recognition due to the increased stability of the heterotypic bond (Fig. 4G). As such, increased homotypic adhesive strength expands the stability of coexistence at the expense of cooperation (Fig. 4E). Furthermore, the adhesive force at which cooperation is maximally stable depends on the shear rate. This provides a possible explanation for the great variability in tandem repeats of *FLO1*, as it allows flexibility in the aggregative strategy to adapt to heterogeneous environments.

DISCUSSION

FLO1 has been identified as a green beard gene governing both aggregation and kin recognition during flocculation [13]. Here, we provide evidence that reciprocity in purely cooperative (homotypic $FLO1^+/FLO1^+$) interactions is associated with increased detachment force compared to exploitative (heterotypic $FLO1^+/flo1^-$) interactions. However, as cooperators are still vulnerable to exploitative interactions, the kin recognition mechanism of Flo1p is permissive and only weakly directs the cooperative benefits to Flo1p-producing individuals. This is in contrast with *FLO11*, which confers homophilic adhesion that leads to direct kin recognition and has been implied in sub-species level discrimination based on a single genetic difference [12]. Our results indicate that varying the relative bond stability of cooperative and exploitative interactions can modulate between both facets of the *FLO1* green beard mechanism: kin recognition and cooperative benefits. We explore shear flow and bond strength, respectively an environmental and intrinsic factor affecting relative bond stability. First, at low shear rate, both cooperative and exploitative interactions are stable resulting in large clusters ($\propto$ cooperative benefits) with low relatedness ($\propto$ kin recognition). High shear rate primarily leads to instability of the exploitative interaction, resulting in smaller clusters but with increased relatedness. Second, the high mobility of tandem repeated sequences of the *FLO1* gene is thought to modulate the adhesive forces between cells [26] and has been shown to result in phenotypic heterogeneity [19]. Assuming the generality of $F_{++} \approx 2\,F_{+-}$, we predict that increasing *FLO1* gene length, and consequently adhesive forces, results in greater cooperative benefits but weaker kin recognition at a given shear rate. We propose that high variability of *FLO1* gene length allows adaptation towards the more appropriate strategy, increasing kin recognition in weak selective regimens or increasing benefits in stringent selection, and thereby potentially stabilizes flocculation in changing environments.

For permissive kin recognition due to the heterophilic nature of Flo1p, we predict a negative-frequency-dependent selection (NFDS) in function of the cooperator frequency. NFDS arises when a decrease in cooperator frequency more severely disadvantages defectors [44]. In our case, decreasing cooperator frequency decreases the probability of defector incorporation in the clusters at favorable locations and decreases the stability of clusters with relatively high defector fractions. This results in a relative increase of cooperator enrichment at low cooperator frequency. In addition, we indicate that in case of homophillic interactions, and thus in the absence of permissiveness in kin recognition, NFDS is lost. Direct kin recognition and the resulting loss of NFDS could be further validated by comparison with *FLO11* in a similar experimental set-up. NFDS is a known driver of biological diversity [45, 46] and it can therefore stabilize the evolution of cooperative phenotypes [44, 47]. In case of permissive kin recognition, we find a stable coexistence of cooperators and defectors in a wide range of cooperation-associated costs and benefits. Coexistence offers flexibility through diversity in environments that are characterized by transient and variable selection pressures, where permissive coming together group formation is thought to outperform staying together [15]. Furthermore, stable coexistence also permits the conservation of variability in *FLO1* gene length, stabilizing the aforementioned adaptability to the environment. Moreover, we postulate that due to the negative-frequency-dependency and the higher return of cooperative benefits, permissive kin recognition is more likely to emerge than direct kin recognition where contacts predominantly originate from stochastic collisions such as low nutrient environments. However, this also renders permissive kin recognition more prone to invasion of defectors.

Our results indicate that permissive CT group formation is susceptible to invasion of non-flocculent phenotypes and can conserve the diversity of a population. Coexistence implies within-group social conflict and is therefore believed to limit the direct further evolution of obligate multicellularity and its accompanied potential of complexity [48]. Nevertheless, we propose that this conserved diversity can facilitate the further evolution of different group formation phenotypes. As such, ST group formation has been shown to emerge in flocculating yeast populations and to synergistically improve population fitness [14, 15]. On longer evolutionary timescales, emerging ST group formation has been shown to be able to outperform CT by flocculation overcoming aforementioned within-group social conflict [15, 49]. Finally, we propose that the physical environment can modulate the significance of permissive CT group formation, thereby shaping the intricate balance between ST and CT, which are fundamental biological operations that can prompt complex biological construction respectively through specialization in obligate multicellularity or conservation of diversity [8, 15].

DATA AVAILABILITY

Data from the single-cell force spectroscopy and flocculation assay have been made available. The simulation code and framework have been made publicly available at https://doi.org/10.5281/zenodo.6472861.

REFERENCES

1. Szathmáry E. Toward major evolutionary transitions theory 2.0. Proc Natl Acad Sci USA. 2015;112:10104–11. https://doi.org/10.1073/pnas.1421398112
2. Niklas KJ, Newman SA. The origins of multicellular organisms. Evol Dev. 2013;15:41–52. https://doi.org/10.1111/ede.12013
3. Pfeiffer T, Bonhoeffer S. An evolutionary scenario for the transition to undifferentiated multicellularity. Proc Natl Acad Sci USA. 2003;100:1095–8. https://doi.org/10.1073/pnas.0335420100
4. Fisher RM, Regenberg B, Multicellular group formation in Saccharomyces cerevisiae. Proc Royal Soc B: Biol Sci. 2019;286. https://doi.org/10.1098/rspb.2019.1098
5. Umen JG. Green algae and the origins of multicellularity in the plant kingdom. Cold Spring Harb Perspect Biol. 2014;6:a016170 https://doi.org/10.1101/cshperspect.a016170

6. Knoll AH. The multiple origins of complex multicellularity. Annu Rev Earth Planet Sci. 2011;39:217–39. https://doi.org/10.1146/annurev.earth.031208.100209
7. Bonner JT. The origins of multicellularity. Integr Biol Issues N. Rev. 1998;1:27–36.
8. Tarnita CE, Taubes CH, Nowak MA. Evolutionary construction by staying together and coming together. J Theor Biol. 2013;320:10–22. https://doi.org/10.1016/j.jtbi.2012.11.022
9. Ratcliff WC, Denison RF, Borrello M, Travisano M. Experimental evolution of multicellularity. Proc Natl Acad Sci USA. 2012;109:1595–1600. https://doi.org/10.1073/pnas.1115323109
10. Koschwanez JH, Foster KR, Murray AW. Sucrose utilization in budding yeast as a model for the origin of undifferentiated multicellularity. PLoS Biol. 2011;9:e1001122 https://doi.org/10.1371/journal.pbio.1001122
11. Kuzdzal-Fick JJ, Chen L, Balázsi G. Disadvantages and benefits of evolved unicellularity versus multicellularity in budding yeast. Ecol Evol. 2019;9:8509–23. https://doi.org/10.1002/ece3.5322
12. Brückner S, Schubert R, Kraushaar T, Hartmann R, Hoffmann D, Jelli E, et al. Kin discrimination in social yeast is mediated by cell surface receptors of the flo11 adhesin family. eLife 2020;9. https://doi.org/10.7554/eLife.55587
13. Smukalla S, Caldara M, Pochet N, Beauvais A, Guadagnini S, Yan C, et al. FLO1 is a variable green beard gene that drives biofilm-like cooperation in budding yeast. Cell. 2008;135:726–37. https://doi.org/10.1016/j.cell.2008.09.037
14. Driscoll WW, Travisano M, Synergistic cooperation promotes multicellular performance and unicellular free-rider persistence. Nat Commun. 2017;8. https://doi.org/10.1038/ncomms15707
15. Pentz JT, Márquez-Zacarías P, Bozdag GO, Burnetti A, Yunker PJ, Libby E, et al. Ecological advantages and evolutionary limitations of aggregative multicellular development. Curr Biol. 2020;30:4155–.e6. https://doi.org/10.1016/j.cub.2020.08.006.
16. Goossens K, Willaert R. Flocculation protein structure and cell-cell adhesion mechanism in Saccharomyces cerevisiae. Biotechnol Lett. 2010;32:1571–85. https://doi.org/10.1007/s10529-010-0352-3
17. Di Gianvito P, Tesnière C, Suzzi G, Blondin B, Tofalo R. FLO5 gene controls flocculation phenotype and adhesive properties in a Saccharomyces cerevisiae sparkling wine strain. Sci Rep. 2017;7:1–12. https://doi.org/10.1038/s41598-017-09990-9
18. Veelders M, Brückner S, Ott D, Unverzagt C, Mösch HU, Essen LO. Structural basis of flocculin-mediated social behavior in yeast. Proc Natl Acad Sci USA. 2010;107:22511–6. https://doi.org/10.1073/pnas.1013210108
19. Verstrepen KJ, Jansen A, Lewitter F, Fink GR. Intragenic tandem repeats generate functional variability. Nat Genet. 2005;37:986–90. https://doi.org/10.1038/ng1618
20. Verstrepen KJ, Klis FM. Flocculation, adhesion and biofilm formation in yeasts. Mol Microbiol. 2006;60:5–15. https://doi.org/10.1111/j.1365-2958.2006.05072.x
21. Verstrepen KJ, Reynolds TB, Fink GR. Origins of variation in the fungal cell surface. Nat Rev Microbiol. 2004;2:533–40. https://doi.org/10.1038/nrmicro927
22. Kraushaar T, Brückner S, Veelders M, Rhinow D, Schreiner F, Birke R, et al. Interactions by the fungal Flo11 adhesin depend on a fibronectin type III-like adhesin domain girdled by aromatic bands. Structure. 2015;23:1005–17. https://doi.org/10.1016/j.str.2015.03.021
23. Chen L, Noorbakhsh J, Adams RM, Samaniego-Evans J, Agollah G, Nevozhay D, et al. Two-dimensionality of yeast colony expansion accompanied by pattern formation. PLoS Comput Biol. 2014;10. https://doi.org/10.1371/journal.pcbi.1003979
24. Oppler ZJ, Parrish ME, Murphy HA, Variation at an adhesin locus suggests sociality in natural populations of the yeast saccharomyces cerevisiae. Proc Royal Soc B: Biol Sci. 2019;286. https://doi.org/10.1098/rspb.2019.1948
25. Lo WS, Dranginis AM. The cell surface flocculin Flo11 is required for pseudohyphae formation and invasion by Saccharomyces cerevisiae. Mol Biol Cell. 1998;9:161–71. https://doi.org/10.1091/mbc.9.1.161
26. El-Kirat-Chatel S, Beaussart A, Vincent SP, Abellán Flos M, Hols P, Lipke PN, et al. Forces in yeast flocculation. Nanoscale. 2015;7:1760–7. https://doi.org/10.1039/c4nr06315e
27. Kobayashi O, Hayashi N, Kuroki R, Sone H. Region of Flo1 proteins responsible for sugar recognition. J Bacteriol. 1998;180:6503–10. https://doi.org/10.1128/jb.180.24.6503-6510.1998
28. Kapsetaki SE, West SA. The costs and benefits of multicellular group formation in algae. Evolution. 2019;73:1296–308. https://doi.org/10.1111/evo.13712
29. Quintero-Galvis JF, Paleo-López R, Solano-Iguaran JJ, Poupin MJ, Ledger T, Gaitan-Espitia JD, et al. Exploring the evolution of multicellularity in Saccharomyces cerevisiae under bacteria environment: An experimental phylogenetics approach. Ecol Evol. 2018;8:4619–30. https://doi.org/10.1002/ece3.3979
30. Goossens KV, Ielasi FS, Nookaew I, Stals I, Alonso-Sarduy L, Daenen L, et al. Molecular mechanism of flocculation self-recognition in yeast and its role in mating and survival. mBio. 2015;6:1–16. https://doi.org/10.1128/mBio.00427-15
31. Hamilton WD. The genetical evolution of social behaviour. I. J Theor Biol. 1964;7:1–16. https://doi.org/10.1016/0022-5193(64)90038-4
32. Queller DC, Ponte E, Bozzaro S, Strassmann JE. Single-gene greenbeard effects in the social amoeba Dictyostelium discoideum. Science. 2003;299:105–6. https://doi.org/10.1126/science.1077742
33. Foty RA, Steinberg MS. The differential adhesion hypothesis: A direct evaluation. Dev Biol. 2005;278:255–63. https://doi.org/10.1016/j.ydbio.2004.11.012
34. Nowak MA. Five rules for the evolution of cooperation. Science. 2006;314:1560–3. https://doi.org/10.1126/science.1133755
35. Nadell CD, Foster KR, Xavier JB. Emergence of spatial structure in cell groups and the evolution of cooperation. PLoS Comput Biol. 2010;6:e1000716 https://doi.org/10.1371/journal.pcbi.1000716
36. Drescher K, Nadell CD, Stone HA, Wingreen NS, Bassler BL. Solutions to the public goods dilemma in bacterial biofilms. Curr Biol. 2014;24:50–55. https://doi.org/10.1016/j.cub.2013.10.030
37. Liu CG, Li ZY, Hao Y, Xia J, Bai FW, Mehmood MA, Computer simulation elucidates yeast flocculation and sedimentation for efficient industrial fermentation. Biotechnol J. 2018;13. https://doi.org/10.1002/biot.201700697
38. Boraas ME, Seale DB, Boxhorn JE. Phagotrophy by flagellate selects for colonial prey: A possible origin of multicellularity. Evol Ecol. 1998;12:153–64. https://doi.org/10.1023/A:1006527528063
39. Staps M, van Gestel J, Tarnita CE. Emergence of diverse life cycles and life histories at the origin of multicellularity. Nat Ecol Evol. 2019;3:1197–205. https://doi.org/10.1038/s41559-019-0940-0
40. De Vargas Roditi L, Boyle KE, Xavier JB. Multilevel selection analysis of a microbial social trait. Mol Syst Biol. 2013;9:684 https://doi.org/10.1038/msb.2013.42
41. Damore JA, Gore J. Understanding microbial cooperation. J Theor Biol. 2012;299:31–41. https://doi.org/10.1016/j.jtbi.2011.03.008
42. Denoth Lippuner A, Julou T, Barral Y. Budding yeast as a model organism to study the effects of age. FEMS Microbiol Rev. 2014;38:300–25. https://doi.org/10.1111/1574-6976.12060
43. Janssens GE, Veenhoff LM. The natural variation in lifespans of single yeast cells is related to variation in cell size, ribosomal protein, and division time. PLoS ONE. 2016;11:e0167394 https://doi.org/10.1371/journal.pone.0167394
44. Ross-Gillespie A, Gardner A, West SA, Griffin AS. Frequency dependence and cooperation: Theory and a test with bacteria. Am Nat. 2007;170:331–42. https://doi.org/10.1086/519860
45. Healey D, Axelrod K, Gore J. Negative frequency-dependent interactions can underlie phenotypic heterogeneity in a clonal microbial population. Mol Syst Biol. 2016;12:877 https://doi.org/10.15252/msb.20167033
46. Harrow GL, Lees JA, Hanage WP, Lipsitch M, Corander J, Colijn C, et al. Negative frequency-dependent selection and asymmetrical transformation stabilise multi-strain bacterial population structures. ISME J. 2021;15:1523–38. https://doi.org/10.1038/s41396-020-00867-w
47. Avilés L. Solving the freeloaders paradox: Genetic associations and frequency-dependent selection in the evolution of cooperation among nonrelatives. Proc Natl Acad Sci USA. 2002;99:14268–73. https://doi.org/10.1073/pnas.212408299
48. Fisher RM, Cornwallis CK, West SA. Group formation, relatedness, and the evolution of multicellularity. Curr Biol. 2013;23:1120–5. https://doi.org/10.1016/j.cub.2013.05.004
49. Pentz JT, Travisano M, Ratcliff WC, Clonal development is evolutionarily superior to aggregation in wild-collected Saccharomyces cerevisiae. In *Artificial Life 14 - Proceedings of the 14th International Conference on the Synthesis and Simulation of Living Systems, ALIFE 2014*, 2014;550–4. 10.7551/978-0-262-32621-6-ch088.
50. Melbinger A, Cremer J, Frey E, The emergence of cooperation from a single mutant during microbial life cycles. J Royal Soc Interface. 2015;12. https://doi.org/10.1098/rsif.2015.0171

ACKNOWLEDGEMENTS

The authors thank Karin Voordeckers for providing us with the yeast strains; Carmen Bartic and Olivier Deschaume for expertise and support with the SCFS experiments. This work was supported by the KU Leuven Research Fund (CELSA/18/031,C24/18/046). B.S. acknowledges support from the Research Foundation Flanders (FWO) grant 12Z6118N. Research in the lab of K.J.V. is supported by KU Leuven, Vlaams Instituut voor Biotechnologie (VIB) and FWO.

AUTHOR CONTRIBUTIONS

HR and BS conceived the project, TB, JP, and BS designed and conducted the simulations. TB designed and conducted the experiments. TB and BS performed data analysis. TB, HS, and BS wrote the manuscript. All authors commented on the manuscript.

FUNDING

This work was supported by the KU Leuven Research Fund (CELSA/18/031, C24/18/046). BS acknowledges support from the Research Foundation Flanders (FWO) grant 12Z6118N. Research in the lab of KJV is supported by KU Leuven, Vlaams Instituut voor Biotechnologie (VIB) and FWO.

COMPETING INTERESTS

The author declares no competing interests.

ADDITIONAL INFORMATION

Supplementary information The online version contains supplementary material available at https://doi.org/10.1038/s41396-022-01275-y.

Correspondence and requests for materials should be addressed to Tom E. R. Belpaire.